Local Magnitude Scale for Earthquakes in the Western Canada Sedimentary Basin, Northeastern British Columbia and Northwestern Alberta

A. Babaie Mahani, Geoscience BC, Vancouver, BC, ali.mahani@mahangeo.com

H. Kao, Natural Resources Canada, Geological Survey of Canada–Pacific, Sidney, BC

Babaie Mahani, A. and Kao, H. (2019): Local magnitude scale for earthquakes in the Western Canada Sedimentary Basin, northeastern British Columbia and northwestern Alberta; *in* Geoscience BC Summary of Activities 2018: Energy and Water, Geoscience BC, Report 2019-2, p. 47–54.

Introduction

Accurate determination of local magnitude (M_L) for induced earthquakes caused by fluid injection is a vital task for regional seismograph network operators in the Western Canada Sedimentary Basin (WCSB). Specific mitigation measures are required by government regulations when the induced events exceed a predefined M_L threshold (Kao et al., 2016). In case of an event with M_L 4.0 or larger, regulators in both British Columbia (BC) and Alberta issue suspension orders to temporarily stop injection operations.

Richter (1935) proposed the first systematic measure of magnitude using a small dataset from earthquakes in southern California. It was based on the maximum zero-to-peak horizontal amplitude of ground displacement, regardless of the wave type, on the Wood-Anderson (WA) torsion seismometer. This method of determining the magnitude is given as

$$M_L = \log(A) - \log(A_0) + S \quad (1)$$

where log (A) is the recorded WA amplitude, in millimetres, whereas $-\log(A_0)$ is the distance correction term for the recorded amplitude. In equation (1), S is a correction term for each station, which is based on the average (over all events) of deviations between M_L at each station and event M_L (Richter, 1935). A positive value for S means that, on average, the station has a higher magnitude than the event magnitude and vice versa. Richter (1935) obtained $-\log(A_0)$ at each distance by defining the zero magnitude at a distance of 100 km. At this distance (ignoring the S term), the ground-motion amplitude is 0.001 mm ($\log(A)$ of –3), therefore $-\log(A_0)$ would be 3. Since 1935, this method has been extensively used around the globe. The aim of this study is to preserve the method's original configuration (the type of sensor and the definition of zero-magnitude), but amend it with region- and station-specific correction terms ($-\log(A_0)$ and S; Savage and Anderson, 1995; Bobbio et al., 2009; Uhrhammer et al., 2011; Ottemoller and Sargeant, 2013; Ristau et al., 2016). To preserve the original sensor type, WA amplitudes are synthetically obtained through deconvolution of the recording sensor's instrument response (non-WA sensors) from the recorded waveform and convolution with the WA-type instrument response.

For WCSB, where widespread oil and gas activities have caused a significant increase in the rate of seismicity in the past decade (Atkinson et al., 2016; Babaie Mahani et al., 2016), Natural Resources Canada (NRCan) follows the original Richter approach to calculate the M_L value of a seismic event with two differences. First, NRCan uses the vertical component instead of the horizontal components (Ristau et al., 2003). Second, a window encompassing the S phase is used and the maximum amplitude within this window is read from the synthetic WA seismograms (Ristau et al., 2003). Even though the static magnification and damping ratio of WA sensors have been found by some researchers to be different than the ones assumed in Richter (1935), NRCan uses the original values. Uhrhammer and Collins (1990) showed that the damping ratio and static magnification of WA sensors are 0.7 and 2080, respectively, which are different than the values of 0.8 and 2800 reported by Anderson and Wood (1925) and used by Richter (1935). Using the static magnification of 2800 instead of 2080 will result in a systematic overestimation of M_L by an average of 0.13 unit (Uhrhammer and Collins, 1990; Bona, 2016). The distance correction term was originally provided for the epicentral distance range of 25–600 km (Richter, 1935), but was later extended to 0 distance by Gutenberg and Richter (1942). The problem with using the epicentral distance is that it ignores the effect of focal depth, resulting in under- and over-estimation at short and large distances (Boore, 1989), and therefore, hypocentral distance is a better distance metric in the modification to the Richter's distance correction term for other regions.

For this study, several distance correction terms, which were obtained for different regions including WCSB, are compared. Using a database of WA amplitudes from small-to-moderate earthquakes in northeastern BC and

This publication is also available, free of charge, as colour digital files in Adobe Acrobat® PDF format from the Geoscience BC website: http://www.geosciencebc.com/s/SummaryofActivities.asp.

northwestern Alberta, a new distance correction term for WCSB is also obtained to maintain NRCan's magnitude estimation routine.

Database and Methodology

The database used in this study includes the vertical component of WA amplitudes from Visser et al. (2017), who compiled a comprehensive earthquake catalogue for WCSB for the period of 2014 to 2016. Over all, there are 4182 events from 39 stations with 18 918 WA amplitudes. Figure 1 shows the distribution of events and seismograph stations and Figure 2a and b shows the event and station M_L versus depth and hypocentral distance, respectively. In Figure 2, the event M_L is the median of the station M_L values. The M_L for each station was calculated from the vertical component of WA amplitudes based on the Richter (1958) distance correction term. For this study, the station M_L values were not corrected for any site/station effect (S in equation 1).

Although depth is a poorly constrained parameter in the regional earthquake catalogues, the maximum depth of the events is ~25 km. Therefore, events are all within the crust (the crust thickness will be determined later in this section). As observed by Yenier (2017) and shown in Figure 2b, the station M_L shows an increasing trend with distance pointing out that the original distance correction term by Richter (1958) is not suitable to account for the regional characteristics of attenuation in WCSB. In Figure 2b the increasing trend in station M_L with distance can be visualized for an individual event: the August 17, 2015 induced event in the northern Montney play of northeastern BC with moment magnitude of 4.6 (star in Figure 2a; Babaie Mahani et al., 2017). Visser et al. (2017) assigned a M_L of 5 for this event.

Figure 3a shows comparison of $-\log(A_0)$ versus hypocentral distance from Richter (1958), Hutton and Boore (1987), Brazier et al. (2008), Bona (2016) and Yenier (2017). Whereas the Richter (1958) and Hutton and Boore (1987) terms are for southern California, Brazier et al. (2008), Bona (2016) and Yenier (2017) terms are for Ethiopia plateau, Italy and WCSB, respectively. These distance correction terms were all obtained for the horizontal component using hypocentral (Hutton and Boore, 1987; Brazier et al., 2008; Yenier, 2017) and epicentral (Richter, 1958; Bona, 2016) distance metrics. Whereas Richter (1958), Hutton and Boore (1987) and Bona (2016) assumed a static magnification of 2800 for the WA sensors, Brazier et al. (2008) and Yenier (2017) used a value of 2080. In Figure 3a, dots represent the observed WA amplitudes, which were normalized based on the reference distance bin 90–110 km. For each distance, amplitudes were divided by the geometric mean of the amplitudes in the reference bin. The data was then forced to pass through 0.001 mm ($-\log(A_0)$ of 3 in Figure 3a) at 100 km distance.

Following Rezapour and Rezaei (2011), a parametric equation for distance correction term can be written as

$$-\log(A_0)=n\times\log\left(\frac{R_{hypo}}{100}\right)+k\times(R_{hypo}-100)+3.0 \quad (2)$$

where R_{hypo} is hypocentral distance, and n and k are the correction for geometrical spreading and an elastic attenuation, respectively.

Equation (2) is written in such a way that for the reference distance of 100 km, amplitudes hold a value of 0.001 mm ($-\log(A_0)$ of 3) to maintain the consistency with the original definition of Richter magnitude. From Figure 3a it is observed that Bona (2016) has the highest correction for n whereas Brazier et al. (2008) has the lowest (note the difference between the slopes of correction terms below

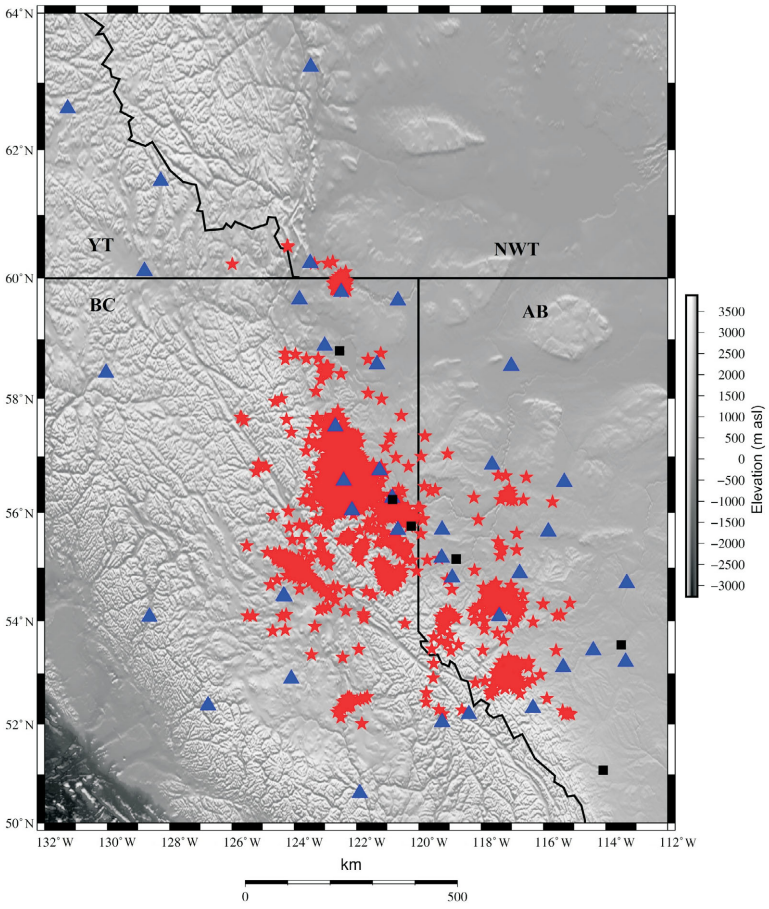

Figure 1. Distribution of earthquakes and seismograph stations from Visser et al. (2017) database used in this study. Stars are the earthquakes, triangles are the stations and squares are the cities and populated areas.

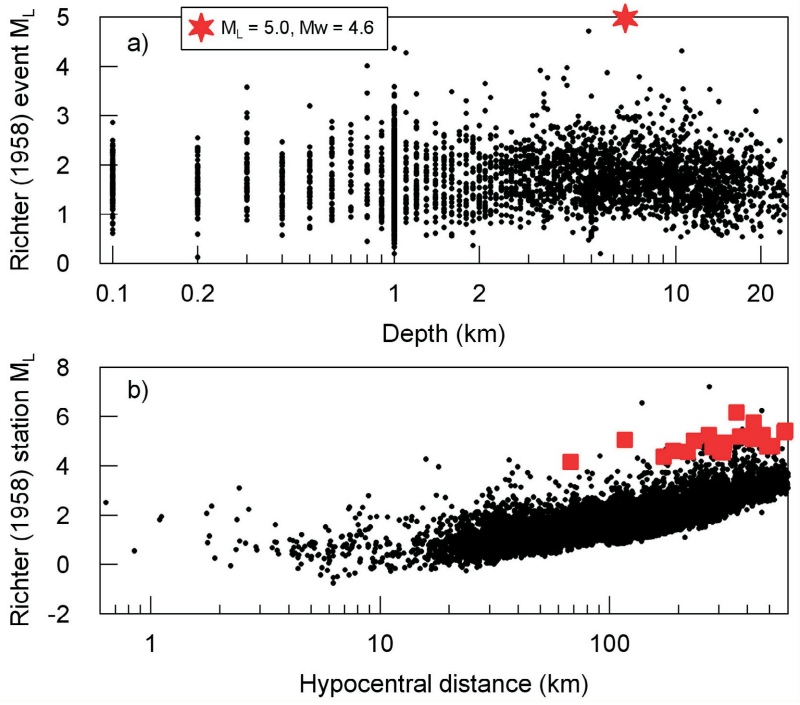

Figure 2. a) Event local magnitude (M_L) versus depth and **b)** station M_L versus hypocentral distance. The M_L values were calculated using the vertical component of Wood-Anderson amplitudes based on the Richter (1958) distance correction term without correcting for the station term (*S* in equation 1). Event M_L is the median of station M_L values. Red star in a) is the August 17, 2015, induced earthquake in the northern Montney play of northeastern British Columbia with moment magnitude (Mw) of 4.6 (Babaie Mahani et al., 2017). Red squares in b) show the station M_L for this event across recording distances.

100 km distance). The *n* is 1.7 for Bona (2016) and 0.7 for Brazier et al. (2008). The effect of *n* on the estimates of M_L can be seen from Figure 3b, which shows the average of the difference between station and event local magnitudes (median from all stations) in equally log-spaced distance bins versus hypocentral distance. Magnitudes were calculated without the *S* term (equation 1). Except Brazier et al. (2008), all other distance correction terms give low station magnitudes at short hypocentral distance (<100 km) and high station magnitudes at hypocentral distance >100 km (Figure 3b). This is important for small-magnitude events as these events are recorded at shorter distances than larger events.

The result of combing and rearranging equations (1) and (2) is

$$\log(A)+3.0=-n\times\log(\frac{R_{hypo}}{100})-k\times(R_{hypo}-100)+M_L-S+\in \quad (3)$$

where $\in$ is the residual (observed minus predicted). The *n*, *k*, M_L and *S* parameters are obtained by constructing the linear inverse equation of d = Gm (Menke, 1984), where d is observed data (log(*A*) + 3.0) and m is the model parameter (*n*, *k*, M_L, *S*) to be determined, G is the kernel matrix that relates d to m. In solving for the model parameters, the correction term for each station (*S*), which represents the overall discrepancy in WA amplitudes between stations located at different site conditions, is obtained simultaneously. Site effects are typically determined relative to a known site condition to avoid trade-offs between source and site terms. In this study, however, site conditions are unknown for the recording stations. Thus, correction factors are computed relative to the average site condition by constraining the *S* terms to attain zero when averaged over all stations. This allows consistent M_L estimations with reduced overall scatter of predictions across different stations (Yenier, 2017).

In determination of $-\log(A_0)$, the most important factor is the shape or functional form of geometrical spreading attenuation, which is characterized by *n*. Although attenuation can be parameterized using a linear, bilinear or trilinear function, Babaie Mahani and Atkinson (2012) found that although the trilinear forms are statistically preferred in many cases, the differences between the forms (linear, bilinear, trilinear) are not sufficiently significant to prefer one over another. For this study, a bilinear function was used to model the distance correction due to geometrical spreading. The bilinear function is simpler because one less parameter needs to be determined in the inversion process yet it is still complex enough to separate direct waves from refracted or head waves travelling along the Moho discontinuity.

Figure 4 shows the P-wave travel time versus epicentral distance, which was obtained by manually picking the onset of the P-wave on the vertical component for selected events with $M_L \geq 3$. Two wave types are shown in Figure 4. The P_g is the direct P-wave, which travels within the crust with velocity v_0, whereas P_n is the head (refracted) P-wave, which travels along the Moho discontinuity with uppermost mantle velocity v_1. From Figure 4, it can be seen that the crossover distance x_D is 200 km. The crossover distance is the distance beyond which the first arrival waves are always head waves. Using the velocities v_0 (6.5 km/s) and v_1 (8.2 km/s), which are the reciprocals of the slope of the direct and head P-wave travel times, and the intercept τ (6.4 s), which is the head P-wave travel time at zero distance, the thickness of the crust (h_0) can be estimated as (Stein and Wysession, 2003)

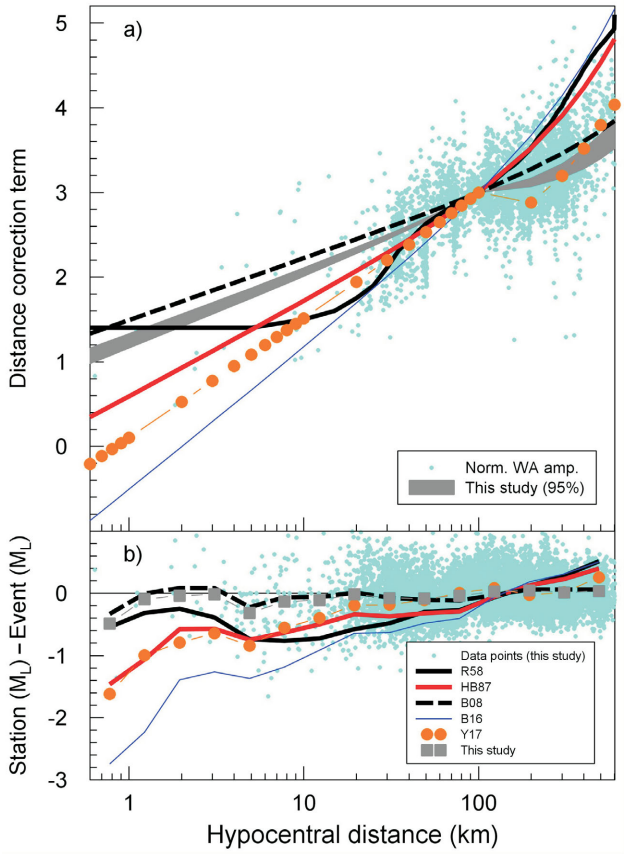

Figure 3. a) Distance correction term [–log(A_0)] versus hypocentral distance. Data is the normalized (Norm.) Wood-Anderson (WA) amplitudes (amp.) in the reference distance bin 90–110 km. Grey area shows the 95% confidence interval for –log(A_0) obtained in this study. **b)** Individual data points for this study and the average of the difference between the station and event local magnitudes (M_L) in equally log-spaced distance bins, using –log(A_0) from Richter (1958), Hutton and Boore (1987), Brazier et al. (2008), Bona (2016), Yenier (2017) and this study, versus hypocentral distance. The M_L values were not corrected for the station term (S in equation 1). Event M_L is the median of station M_L values. Abbreviations: B08, Brazier et al. (2008); B16, Bona (2016); HB87, Hutton and Boore (1987); R58, Richter (1958); Y17, Yenier (2017).

$$h_0 = \frac{\tau}{2\times\sqrt{\left(\frac{1}{v_0^2}\right)-\left(\frac{1}{v_1^2}\right)}} \quad (4)$$

Equation (4) gives 33 km for the thickness of the crust. The critical distance x_c, below which the head waves disappear, is obtained as (Stein and Wysession, 2003)

$$x_c = 2\times h_0 \times \frac{v_0/v_1}{\sqrt{1-\left(\frac{v_0^2}{v_1^2}\right)}} \quad (5)$$

In this case, x_c is 85 km. Therefore, the bilinear function of the form

$$\begin{cases} b_1\times\log\left(\frac{R_{hypo}}{100}\right) & R_{hypo}\le 85 \text{ km} \\ b_2\times\log\left(\frac{R_{hypo}}{100}\right) & R_{hypo}> 85 \text{ km} \end{cases} \quad (6)$$

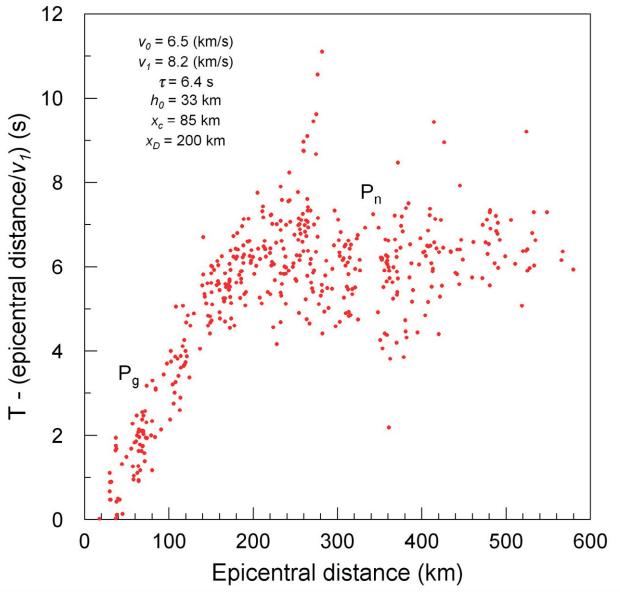

Figure 4. Reduced P-wave travel time versus epicentral distance. Abbreviations: h_0, crust thickness; P_g, direct P-wave; P_n, head (refracted) P-wave; τ, intercept; T, time; v_0, velocity of direct P-wave within the crust; v_1, velocity of head P-wave within the mantle; x_c, critical distance; x_D, crossover distance.

was used to model the effect of geometrical spreading, n, where b_1 and b_2 are the coefficients to be determined.

Distance Correction Term for WCSB

Using the equations (3) and (6), model parameters (b_1, b_2, k, M_L, S) were obtained through the maximum likelihood estimation. For this study, only those events with at least five observations were used (1586 events with 12 000 WA amplitudes). Figure 5 shows ∈ versus hypocentral distance and event M_L (median of station M_L values based on Richter [1958] distance correction term and without the S term). Although data is sparse at close distances (R_{hypo} <10 km) and larger magnitudes (M_L >4), there are no trends in the residuals with distance or magnitude, which means that the inversion was successful assuming the functional forms for the attenuation and geometric spreading. Therefore, in this study, the distance correction term, –log(A_0), for WCSB is

$$\begin{cases} 0.7974\times\log\left(\frac{R_{hypo}}{100}\right)+0.0016\times(R_{hypo}-100)+3.0 & R_{hypo}\le 85 \text{ km} \\ -0.1385\times\log\left(\frac{R_{hypo}}{100}\right)+0.0016\times(R_{hypo}-100)+3.0 & R_{hypo}> 85 \text{ km} \end{cases} \quad (7)$$

Overall, the distance correction term (equation 7) appears to work well at all distances and is similar to Brazier et al. (2008; Figure 3).

Figure 6 shows event M_L (median of station M_L without the S term) computed with the distance correction term obtained in this study versus Richter (1958), Hutton and Boore (1987), Brazier et al. (2008), Bona (2016) and Yenier

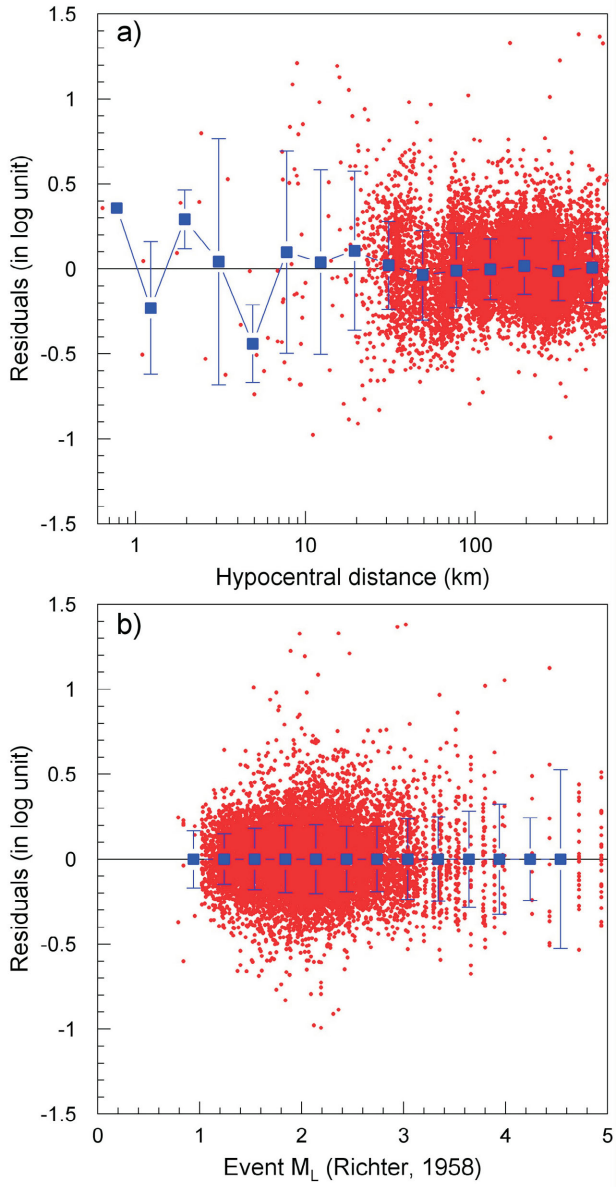

Figure 5. Residuals (observed minus predicted) of the inversion process versus **a)** hypocentral distance and **b)** event local magnitude (M_L). Squares are the mean of residuals in equally log-spaced distance bins and equally linear-spaced magnitude bins and the error bars are one standard deviation. The M_L values were calculated using the vertical component of Wood-Anderson amplitudes based on the Richter (1958) distance correction term without correcting for the station term (*S* in equation 1). Event M_L is the median of station M_L values.

(2017). The AVR_M in Figure 6 is the average of the difference between M_L values (M_L from another study minus M_L from this study). Overall, M_L values from this study are lower than those obtained using $-\log(A_0)$ of Richter (1958), Hutton and Boore (1987), Brazier et al. (2008) and Bona (2016) but higher than Yenier (2017).

To further analyze the difference between M_L values, the event M_L was calculated from station M_L (median of station magnitudes without the *S* term) at different distance bins ($R_{hypo} \leq 50$ km, 50 km $< R_{hypo} \leq 100$ km, 100 km $< R_{hypo} \leq 200$ km, $R_{hypo} > 200$ km) using the distance correction terms obtained in this study and Yenier (2017). In Figure 7, the difference between M_L values (M) from Yenier (2017) and this study is plotted against M_L values from this study. Also plotted are the averages of M in equally linear-spaced magnitude bins. The largest deviation between this study's M_L values and Yenier (2017) values occurs when all stations are below 50 km for which the M_L values from Yenier (2017) are lower by an average of 0.27 unit. For larger distance bins, the values are more similar. The lower M_L values from Yenier (2017) at short distances are due to the fact that Yenier (2017) assigned a higher rate for the geometrical attenuation of ground-motion amplitudes for distances <100 km (1.4 for Yenier [2017] versus 0.8 in this study).

Conclusions

Determination of an accurate local magnitude (M_L) for induced earthquakes requires adjustments to the region-specific distance correction term, $-\log(A_0)$, in Richter's (1935) magnitude equation. When the maximum magnitude of induced events is close to the threshold set by regulators to suspend injections, having an accurate M_L can have important economic consequences for operators. For this reason, a comprehensive catalogue of Wood-Anderson amplitudes from earthquakes in the Western Canada Sedimentary Basin (WCSB) was used to analyze the $-\log(A_0)$ term previously obtained for WCSB and several other regions. By assuming a bilinear model for the attenuation of ground-motion amplitudes, a new formula of $-\log(A_0)$ was obtained specifically for monitoring induced seismicity in WCSB using Natural Resources Canada's M_L calculation routine. This study's correction term for distance is

$$\begin{cases} 0.7974\times\log\left(\frac{R_{hypo}}{100}\right)+0.0016\times(R_{hypo}-100)+3.0 & R_{hypo}\leq 85 \text{ km} \\ -0.1385\times\log\left(\frac{R_{hypo}}{100}\right)+0.0016\times(R_{hypo}-100)+3.0 & R_{hypo}> 85 \text{ km} \end{cases}$$

where R_{hypo} is the hypocentral distance. This study's distance correction term results in lower M_L values by an average of 0.29, 0.27, 0.12 and 0.34 units compared to those obtained by Richter (1958; California), Hutton and Boore (1987; California), Brazier et al. (2008; Ethiopia plateau) and Bona (2016; Italy), respectively, when all distance ranges are considered. However, it gives higher M_L values than those obtained by Yenier (2017; WCSB) by an average of 0.12 unit over the distance range of 0 to 600 km. When comparing this study to Yenier's (2017) study, this difference in M_L varies with R_{hypo}: 0.27 unit for $R_{hypo} \leq 50$ km, 0.08 unit for 50 km $< R_{hypo} \leq 100$ km, 0.12 for 100 km $< R_{hypo} \leq 200$ km, and 0.10 for $R_{hypo} > 200$ km.

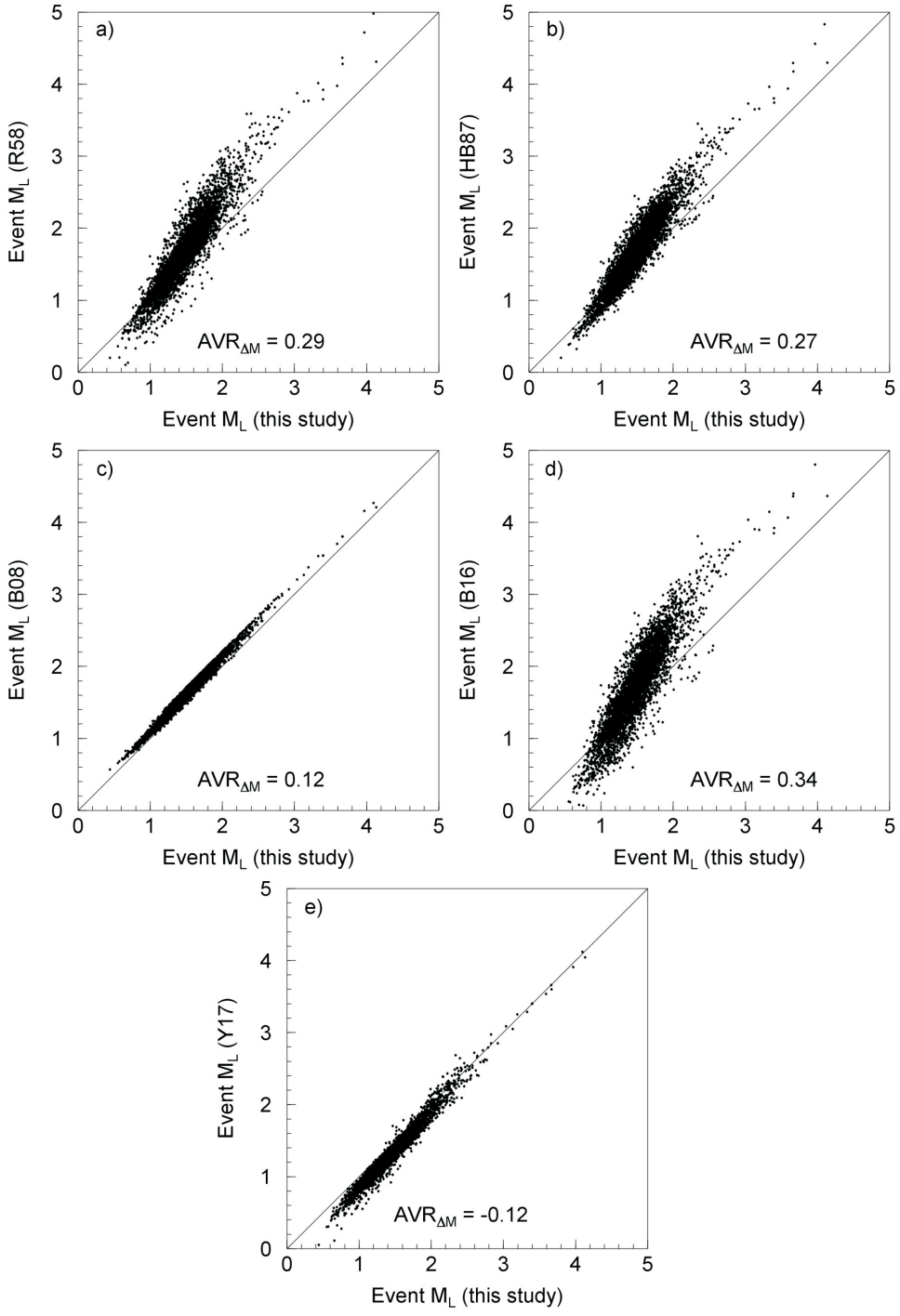

Figure 6. Event local magnitude (M_L) computed from the distance correction terms obtained in this study versus those obtained by **a)** Richter (1958; R58); **b)** Hutton and Boore (1987; HB87); **c)** Brazier et al. (2008; B08); **d)** Bona (2016; B16); and **e)** Yenier (2017; Y17). The AVR_M is the average deviation of M_L values (M_L from another study minus M_L from this study). The solid lines show the 1:1 agreement of magnitude estimates. The M_L values were not corrected for the station term (*S* in equation 1). Event M_L is the median of station M_L values.

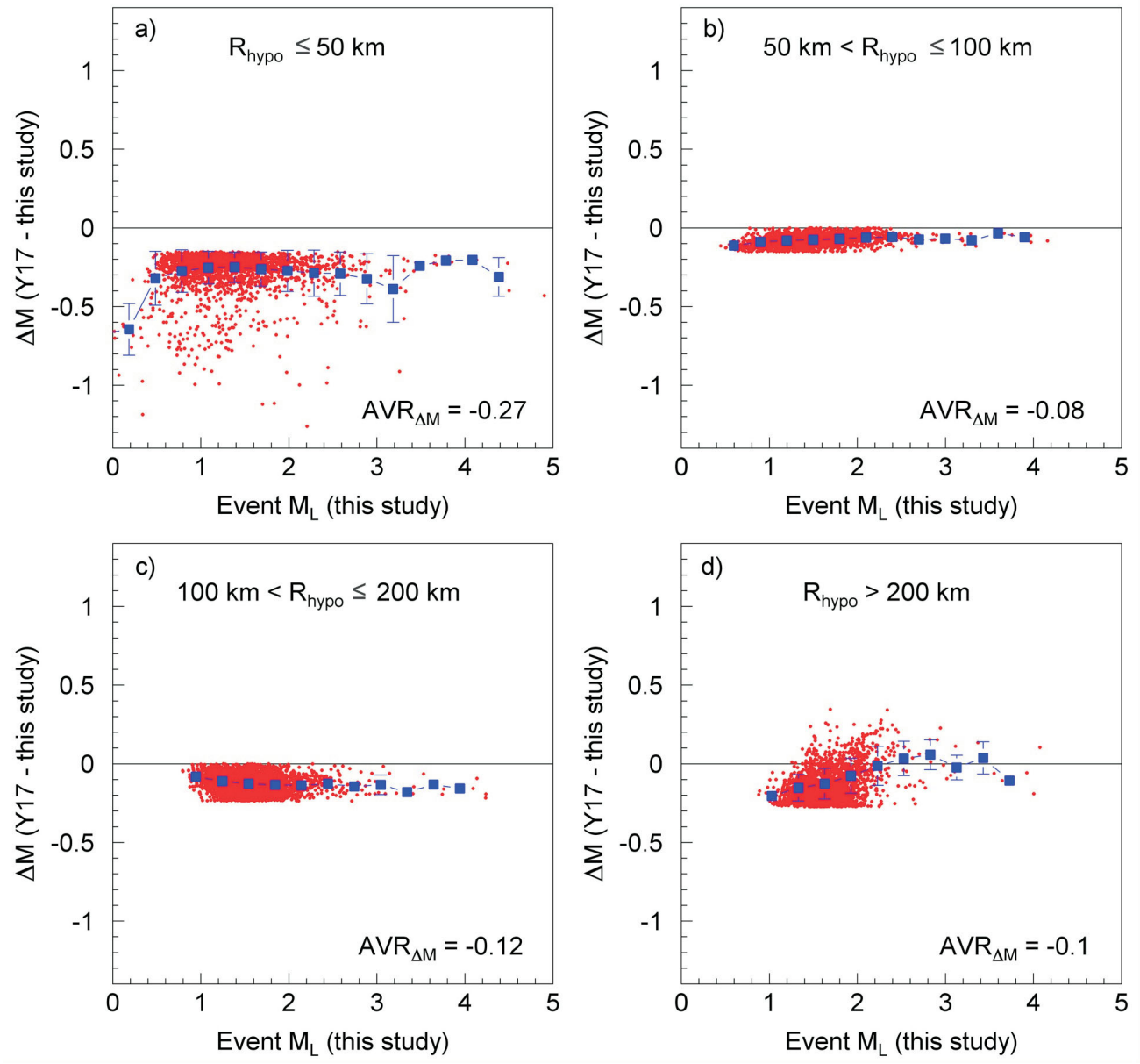

Figure 7. Difference (M) between event local magnitudes (M_L) computed from the distance correction terms obtained in this study versus those obtained by Yenier (2017; Y17) using stations in different hypocentral distance (R_{hypo}) bins: **a)** $R_{hypo} \leq 50$ km; **b)** 50 km < $R_{hypo} \leq 100$ km; **c)** 100 km < $R_{hypo} \leq 200$ km; and **d)** $R_{hypo} > 200$ km. The AVR_M is the average deviation of M_L values (M_L from Yenier [2017] study minus M_L from this study). The solid lines show the 1:1 agreement of magnitude estimates. Squares are the averages of M in equally linear-spaced magnitude bins with the error bars showing one standard deviation. The M_L values were not corrected for the station term (S in equation 1). Event M_L is the median of station M_L values.

Acknowledgments

The authors would like to thank R. Visser for providing the Wood-Anderson amplitudes and comments on the Natural Resources Canada magnitude calculation. Also thanked is E. Yenier for his explanations regarding the inversion process. This project was partially supported by BC Seismic Research Consortium (Geoscience BC, BC Oil and Gas Research and Innovation Society, Canadian Association of Petroleum Producers, BC Oil and Gas Commission, Yukon Geological Survey). The authors appreciate comments by Seismological Research Letters' Z. Peng, and three anonymous reviewers who helped improve the manuscript.

Natural Resources Canada, Lands and Minerals contribution 20180221

References

Anderson, J.A. and Wood, H.O. (1925): Description and theory of the torsion seismometer; Bulletin of the Seismological Society of America, v. 15, p. 1–72.

Atkinson, G.M., Eaton, D., Ghofrani, H., Walker, D., Cheadle, B., Schultz, R., Scherbakov, R., Tiampo, K., Gu, Y.J., Harrington, R., Liu, Y., van der Baan, M. and Kao, H. (2016): Hydraulic fracturing and seismicity in the Western Canada Sedimentary Basin; Seismological Research Letters, v. 87, p. 631–647.

Babaie Mahani, A. and Atkinson, G.M. (2012): Evaluation of functional forms for the attenuation of small-to-moderate-earthquake response spectral amplitudes in North America; Bulletin of the Seismological Society of America, v. 102, p. 2714–2726.

Babaie Mahani, A., Kao, H., Walker, D., Johnson, J. and Salas, C. (2016): Performance evaluation of the regional seismograph network in northeast British Columbia, Canada, for monitoring of induced seismicity; Seismological Research Letters, v. 87, p. 648–660.

Babaie Mahani, A., Schultz, R., Kao, H., Walker, D., Johnson, J. and Salas, C. (2017): Fluid injection and seismic activity in the northern Montney Play, British Columbia, Canada, with special reference to the 17 August 2015 Mw 4.6 induced earthquake; Bulletin of the Seismological Society of America, v. 107, p. 542–552.

Bobbio, A., Vassallo, M. and Festa, G. (2009): A local magnitude scale for southern Italy; Bulletin of the Seismological Society of America, v. 99, p. 2461–2470.

Bona, M.D. (2016): A local magnitude scale for crustal earthquakes in Italy; Bulletin of the Seismological Society of America, v. 106, p. 242–258.

Boore, D.M. (1989): The Richter scale: its development and use for determining earthquake source parameters; Tectonophysics, v. 166, p. 1–14.

Brazier, R.A., Miao, Q., Nyblade, A.A., Ayele, A. and Langston, C.A. (2008): Local magnitude scale for the Ethiopia plateau; Bulletin of the Seismological Society of America, v. 98, p. 2341–2348.

Gutenberg, B. and Richter, C.F. (1942): Earthquake magnitude, intensity, energy, and acceleration; Bulletin of the Seismological Society of America, v. 32, p. 163–191.

Hutton, L.K. and Boore, D.M. (1987): The ML scale in southern California; Bulletin of the Seismological Society of America, v. 77, p. 2074–2094.

Kao, H., Eaton, D.W., Atkinson, G.M., Maxwell, S. and Babaie Mahani, A. (2016): Technical meeting on the traffic light protocols (TLP) for induced seismicity: summary and recommendations; Geological Survey of Canada, Open File 8075, 20 p.

Menke, W. (1984): Geophysical Data Analysis: Discrete Inverse Theory; Academic Press, San Diego, California, 289 p.

Ottemoller, L. and Sargeant, S. (2013): A local magnitude scale for the United Kingdom; Bulletin of the Seismological Society of America, v. 103, p. 2884–2893.

Rezapour, M. and Rezaei, R. (2011): Empirical distance attenuation and the local magnitude scale for northwest Iran; Bulletin of the Seismological Society of America, v. 101, p. 3020–3031.

Richter, C.F. (1935): An instrumental earthquake magnitude scale; Bulletin of the Seismological Society of America, v. 25, p. 1–31.

Richter, C.F. (1958): Elementary Seismology; W.H. Freeman and Co., San Francisco, California, 578 p.

Ristau, J., Harte, D. and Salichon, J. (2016): A revised local magnitude (ML) scale for New Zealand earthquakes; Bulletin of the Seismological Society of America, v. 106, p. 398–407.

Ristau, J., Rogers, G.C. and Cassidy, J.F. (2003): Moment magnitude-local magnitude calibration for earthquakes off Canada's west coast; Bulletin of the Seismological Society of America, v. 93, p. 2296–2300.

Savage, M.K. and Anderson, J.G. (1995): A local-magnitude scale for the western Great Basin–eastern Sierra Nevada from synthetic Wood-Anderson seismograms; Bulletin of the Seismological Society of America, v. 85, p. 1236–1243.

Stein, S. and Wysession, M. (2003): An Introduction to Seismology, Earthquakes, and Earth Structure; Blackwell Publishing, Malden, Massachusetts, 512 p.

Uhrhammer, R.A. and Collins, E.R. (1990): Synthesis of Wood–Anderson seismograms from broadband digital records; Bulletin of the Seismological Society of America, v. 80, p. 702–716.

Uhrhammer, R.A., Hellweg, M., Hutton, K., Lombard, P., Walters, A.W., Hauksson, E. and Oppenheimer, D. (2011): California integrated seismic network (CISN) local magnitude determination in California and vicinity; Bulletin of the Seismological Society of America, v. 101, p. 2685–2693.

Visser, R., Smith, B., Kao, H., Babaie Mahani, A., Hutchinson, J. and McKay, J.E. (2017): A comprehensive earthquake catalogue for northeastern British Columbia and western Alberta, 2014-2016; Geological Survey of Canada, Open File 8335, 28 p.

Yenier, E. (2017): A local magnitude relation for earthquakes in the Western Canada Sedimentary Basin; Bulletin of the Seismological Society of America, v. 107, p. 1421–1431.